(2)

AR-006-336

AD-A236 067

91-01062

A One-Dimensional Flux-Corrected Transport Code for Detonation Calculations

D.A. Jones, E.S. Oran * *and R. Guirguis*†

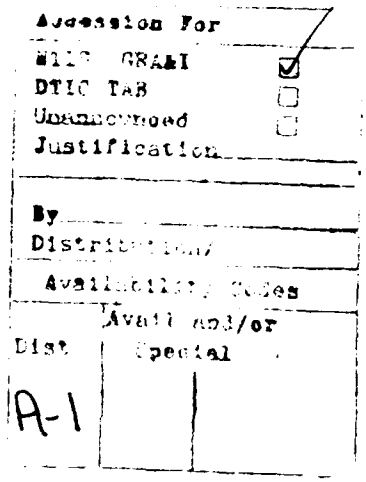

MRL Research Report
MRL-RR-2-90

Abstract

The development of a one-dimensional Flux-Corrected Transport code to model detonation in a homogeneous medium is described. The material flow is modelled using the Euler equations, and the chemical kinetics by a two-step induction parameter model which uses a quasi-steady induction time and first order Arrhenius kinetics. Two different modes of initiation are compared. Conditions necessary for a self-sustaining detonation are described and illustrated. A detailed comparison is made between the variable profiles calculated by the code and those calculated analytically using the simple Chapman-Jouguet theory and self-similar analysis, and the overall agreement is excellent. The effect of the computational cell size on these solutions is also considered.

* *Naval Research Laboratory, Washington DC 20375, USA*
† *Naval Surface Warfare Center, Silver Spring, MD 20903, USA*

MATERIALS RESEARCH LABORATORY

Published by

DSTO Materials Research Laboratory
Cordite Avenue, Maribyrnong,
Victoria, 3032 Australia

Telephone: (03) 319 3887
Fax: (03) 318 4536

AR No. 006-336

Authors

David Jones

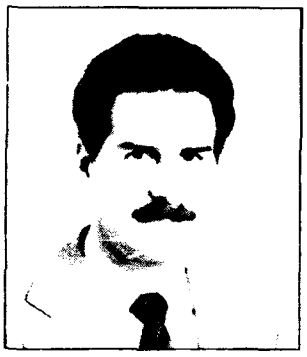

David Jones graduated from Monash University in 1972 with a BSc (Hons). He obtained his PhD from Monash in 1976. After working at Strathclyde University, London University and the University of New South Wales he joined MRL in 1983. He has worked on the numerical modelling of shaped charge warheads and slapper detonator devices. From February 1987 to May 1988 he was a Visiting Scientist at the Laboratory for Computational Physics and Fluid Dynamics at the Naval Research Laboratory in Washington DC. While there he worked on advanced computational fluid dynamics.

Elaine S. Oran

Elain Oran works at the Naval Research Laboratory in the Laboratory for Computational Physics, Washington, DC.

Raafat Guirguis

Raafat Guirguis is employed by Naval Surface Warfare Center, White Oak, Maryland.

Contents

A One-Dimensional Flux-Corrected Transport Code for Detonation Calculations

1. Introduction

A detonation wave is a supersonic shock wave travelling through a reactive medium. The high temperature generated by the passage of the shock through the material initiates chemical reaction and energy release. A stable detonation with a unique detonation velocity will develop if the chemical reaction zone can remain coupled to the wave and continuously feed energy to the shock front. Numerical simulations of propagating detonations therefore require simultaneous solutions of equations which describe both the material flow and reaction kinetics.

Good reviews of the early work on the numerical simulation of detonation can be found in the books by Mader [1] and Fickett and Davis [2]. One of the first calculations was reported by Hubbard and Johnson [3]. Most of this early work relied on the artificial viscosity method of von Neumann and Richtmyer [4] to model shock formation, although one exception was the work of Fickett and Wood [5], which used a method-of-characteristics code to model one-dimensional longitudinal instabilities in overdriven detonations. Codes which are based on the method-of-characteristics technique have the advantage of very accurately resolved shock fronts, but they are not very easily extended into two dimensions. Conversely, codes based on the artificial viscosity method are readily extended to two or three dimensions, but they have the disadvantage of smearing the shock front over several cells. Artificial viscosity codes also cause problems when coupled to modern schemes which model the reaction kinetics of heterogeneous condensed phase explosives. Many of these schemes incorporate a material viscosity term to model hot spot formation [6], and the identification of the correct value of this term is often complicated by the smearing of the shock front caused by the artificial viscosity. This problem has been noted in a recent MRL report [7].

Advances in computational fluid dynamics during the 1970s have removed the need for reliance on the artificial viscosity method for two or three-dimensional shock calculations. The Flux-Corrected Transport (FCT) technique developed by Boris and Book [8-10] showed that nonlinear monotone methods could accurately

resolve shock fronts to within one cell width without the need for an additional artificial viscosity term. Since then a variety of non-linear methods have been derived and applied extensively to gas dynamic and fluid calculations. The paper by Sod [11] provides a good review of some of these methods. In general, however, the explosives community has been slow in applying these techniques to the numerical simulation of detonation phenomena. One exception to this is the reactive flow work of Oran and collaborators at the Naval Research Laboratory. They have used one and two-dimensional FCT codes to model both gaseous detonation [12, 13] and homogeneous condensed phase detonations [14-16]. A comprehensive review of this work has recently been published by Oran and Boris [17]. Nunziato and Baer have also used FCT methods to model flame propagation and growth to detonation in multiphase flows [18], and Thomas has also used FCT codes for detonation calculations [19].

MRL is interested in the shock initiation of heterogeneous condensed phase explosives. A previous MRL report [7] has critically reviewed models for the shock initiation of these materials and their suitability for implementation in various hydrocodes. This report describes a one-dimensional FCT computer code which models the propagation of detonation in homogeneous materials with a polytropic equation of state. The decomposition of the material is described by first-order kinetics with an Arrhenius temperature dependence. A pressure and temperature dependent induction time is also included. Replacement of the polytropic equation of state with one more suited to condensed phase materials, and implementation of one of the schemes described in [7], would then allow the code to model shock initiation of heterogeneous explosives. The code is similar to those described in broad outline in [17], and in more detail in [14]. In this report we present a more detailed description of some aspects of the model and its numerical solution. We make a detailed comparison between the variable profiles calculated by the code and those calculated analytically using the simple Chapman-Jouguet (CJ) theory, and we also consider the effect of the computational cell size on these solutions. Finally, we illustrate the use of the code by discussing its application to recent work on detonation in a stoichiometric mixture of hydrogen and oxygen.

2. *The Physical Model*

The numerical simulation of detonation requires the simultaneous solution of the coupled equations describing material flow and chemical reaction. The pressures generated by the detonation of a condensed phase explosive are so high (typically a few hundred kilobars) that material strength may be neglected, and the appropriate equations describing the material flow are those of reactive fluid dynamics [20]. We also make the usual assumption that energy transport by heat conduction, viscosity, and radiation is negligibly small compared with transport by motion [2]. In this case, the appropriate fluid equations are the Euler equations, a set of three coupled partial differential equations describing the conservation of mass, momentum, and energy. In a one-dimensional cartesian coordinate system, these are

$$\frac{\partial \rho}{\partial t} + \frac{\partial (\rho v)}{\partial x} = 0 \qquad (1)$$

$$\frac{\partial (\rho v)}{\partial t} + \frac{\partial (\rho v^2)}{\partial x} = - \frac{\partial P}{\partial x} \qquad (2)$$

$$\frac{\partial E}{\partial t} + \frac{\partial (Ev)}{\partial x} = - \frac{\partial (Pv)}{\partial x} \qquad (3)$$

where t denotes time, x the spatial coordinate, ρ the density, v the fluid (or particle) velocity, and P the pressure. The quantity E is the total energy per unit volume and is defined by

$$E = \rho e + 0.5 \rho v^2 \qquad (4)$$

where e is the specific internal energy (including the stored chemical energy).

The thermodynamic properties of a nonreacting material are completely specified by the fundamental equation, which expresses the internal energy of the system in terms of its entropy, volume, and mole numbers. The partial derivatives of the fundamental equation with respect to its dependent variables then define the equations of state of the material [21]. The thermodynamic state can also be specified precisely if **all** the equations of state of the system are known. For a simple single-component system there are three equations of state. Only two of these need to be specified however as the Gibbs-Duhem relation may always be used to obtain the third equation [21]. The two equations of state normally specified are the mechanical equation of state and the caloric equation of state, which have the forms

$$P = P(e, \rho)$$

$$T = T(e, \rho)$$

where T is the temperature of the material. We use a polytropic model for our fluid, which describes an ideal gas for which the ratio of specific heats at constant pressure and temperature is a constant. The equations of state are then given by [22],

$$P = (\gamma - 1)\rho e \tag{5}$$

$$T = \frac{e}{c_v} \tag{6}$$

where $\gamma = c_p/c_v$, and c_p and c_v are the specific heats at constant pressure and volume respectively. Equations (5) and (6) can also be combined to give

$$P = \rho RT \tag{7}$$

in which R is the specific gas constant, $R = R^*/mw$, where R^* is the universal gas constant and mw is the molecular weight of the fluid.

The material is allowed to undergo a single irreversible chemical reaction, represented schematically by

$$explosive\ reactants \rightarrow explosive\ products \tag{8}$$

The condition that both the molecular weight and γ remain unaltered during the progress of the reaction is also imposed. The chemical composition at any time is described by the progress variable w, which we define to be the explosive mass fraction, i.e.

$$w = \frac{mass\ of\ reactants}{mass\ of\ reactants + mass\ of\ products} \tag{9}$$

w therefore goes from one to zero as the reaction proceeds from pure reactants to pure products. The temperature increase as the reaction proceeds is calculated from

$$T = \frac{(e - w\Delta E)}{c_v} \tag{10}$$

where ΔE is the heat of reaction. The pressure is then calculated from equation (7). This is a commonly used energetic scheme in detonation calculations [23].

The chemical reaction represented schematically by equation (8) often takes place in two distinct stages. In the first step, the explosive fuel is converted into

5. Results for Stoichiometric H_2/O_2

radicals by a series of endothermic processes. During this step, the concentration of radicals steadily increases but remains so small that the amount of fuel consumed and products produced can be neglected, and there is no apparent rise in either temperature or pressure. We allow for this induction period by the explicit introduction of an induction time τ^o. Induction times are measured at constant temperature and pressure, and we use a superscript zero to denote that τ^o is the induction time measured (or calculated) under these conditions. In the course of our calculations, however, a given control volume may undergo a series of temperature and pressure changes and the true induction time τ will not necessarily be equal to τ^o. Therefore τ is determined from the solution of the integral equation

$$\int_o^{\tau} \frac{dt}{\tau^o(T,P)} = 1 \qquad (11)$$

This formula provides a convenient way of averaging over changing temperature and pressure during the chemical induction period, and reduces automatically to the correct induction delay when the pressure and temperature are constant.

We also introduce an induction parameter f, which represents the fraction of induction time already elapsed. f is obtained from the solution of the equation

$$\frac{df}{dt} = \frac{1}{\tau^o(T,P)} \qquad (12)$$

where $f(o) = o$. Energy release is then initiated when $f = 1$. A useful expression for τ^o which has been used previously [16] has the form

$$\tau^o(T,P) = A_\tau \exp(E_\tau/RT)\ \frac{P_o}{P} \qquad (13)$$

where P_o is a reference pressure.

When the induction time has elapsed, the energy release is assumed to follow first order kinetics with an Arrhenius temperature dependence

$$\frac{dw}{dt} = -wA_r \exp(-E_r/RT), \qquad (14)$$

where E_r is the activation energy and A_r is the frequency factor. Values for the constants A_τ, E_τ and A_r, E_r can be found from solutions of the detailed chemical kinetic equations if the full reaction scheme is known [13], or else fitted to

experimental measurements [15]. The combination of an induction parameter model of the form of equation (12) and reaction rate dependence given by equation (14) was first described by Oran et al. [24].

For some reactive compositions, both the induction time and reaction rate are independent of temperature and pressure in the region of interest and can be taken as constants. We describe one example of this in a later section where we develop a simple model for the detonation of a stoichiometric mixture of hydrogen and oxygen.

When the reaction occurs in a fluid moving with a velocity v, the time derivatives in equations (12) and (14) denote a derivative following the fluid flow and the equations become

$$\frac{\partial f}{\partial t} + v\frac{\partial f}{\partial x} = \frac{1}{\tau^o} \tag{15}$$

and

$$\frac{\partial w}{\partial t} + v\frac{\partial w}{\partial x} = -wA_r \exp(-E_r/RT) \tag{16}$$

respectively. Equations (15) and (16) can then be combined with the continuity equation, equation (1), to give

$$\frac{\partial(\rho f)}{\partial t} + \frac{\partial(\rho f v)}{\partial x} = \frac{\rho}{\tau^o} \tag{17}$$

and

$$\frac{\partial(\rho w)}{\partial t} + \frac{\partial(\rho w v)}{\partial x} = -\rho wA_r \exp(-E_r/RT) \tag{18}$$

Equations (17) and (18) are now in conservation form and can be solved by the same method used to solve equations (1) through (3).

In the numerical solution procedure outlined in the next section, equation (17) is modified slightly to convect the product wf rather than f alone, i.e. equation (17) is replaced by

$$\frac{\partial (\rho\, wf)}{\partial t} + \frac{\partial (\rho\, wfv)}{\partial x} = \frac{w\rho}{\tau^o} \qquad (19)$$

which is equivalent to writing equation (12) in the form

$$\frac{d(wf)}{dt} = \frac{w}{\tau^o} \qquad (20)$$

The replacement of equation (17) by equation (19) facilitates calculations in cells containing fractions of both products and reactants. Equation (14) ensures that any products in a mixed cell have no effect on the reaction of the remaining unreacted explosive. The reasoning behind the replacement of equation (17) by equation (19) is complex, but is explained in detail in reference [15].

3. *Numerical Solution*

The computer code RSHOCK solves equations (1), (2), (3), (18) and (19) using the FCT subroutine JPBFCT (a computer listing of RSHOCK may be obtained from D.A. Jones on request). Operator splitting is used for the chemical source terms in equations (18) and (19), and equations (4), (7) and (10) define the additional thermodynamic variables in terms of the convected quantities. JPBFCT is a slightly modified version of the subroutine ETBFCT, which is described in detail in reference [25]. This multiple entry subroutine solves generalised continuity equations of the form

$$\frac{\partial \rho}{\partial t} + \frac{1}{r^{\alpha-1}} \frac{\partial}{\partial r} (r^{\alpha-1}\, \rho\, v) = \frac{1}{r^{\alpha-1}} \frac{\partial}{\partial r} (r^{\alpha-1}\, D_1) + C_2 \frac{\partial D_2}{\partial r} + D_3 \qquad (21)$$

using an algorithm which gives fourth order accurate phases and minimal residual diffusion. The routine can treat cartesian, cylindrical or spherical one-dimensional systems for $\alpha = 1, 2, 3$ respectively.

The solution procedure for the coupled set of equations is to first call JPBFCT to convect the density ρ. Next, the subroutine SOURCD is called to calculate the source term for the momentum equation, and then JPBFCT is called to convect the product ρv. SOURCD is then called again to calculate the source term for the energy equation, and then JPBFCT called to advance the total energy E. This procedure is performed twice for each hydrodynamic time step Δt. On the first pass, the variables ρ, ρv and E are advanced over a time $0.5\ \Delta t$, and are then used to calculate the source terms at this intermediate time. On the second pass the variables are convected over the full step Δt using the source term values evaluated at the half step. This procedure greatly increases the accuracy of the simulation by correcting a phase lag in the values of the variables which occurs as the equations are solved sequentially. The variables ρw and ρwf are also convected during this sequence, with the source terms on the right side of equations (18) and (19) set to zero. Only ρw is convected on the half step cycle because the pressure depends on w, but not f. On the full step calculation, both w and f are convected. At the completion of the transport stage, e, T and P are then calculated from equations (4), (6) and (7).

Next, the program checks to see if the induction time has elapsed by calculating the variable DT, which is equal to the amount of time remaining before f equals one. At this stage, there are two possibilities, DT is either greater or less than the hydrodynamic time step Δt. The former case implies that no burning occurs at the end of the time step, and so the time dependent part of equation (19) is solved via the explicit equation

$$(wf)^{new} = (wf)^{old} + \Delta t\, w^{old}/\tau \tag{22}$$

to update f, and w remains fixed at one. The latter case implies that burning starts before the end of the current time step. The quantity DT is then reset to the burn time within the time step, i.e. $DT = \Delta t - DT$, and w is updated by the implicit solution of the time dependent part of equation (18),

$$w^{new} = w^{old}/(1 + A_r \exp(-E_r/RT)DT) \tag{23}$$

Equations (10) and (7) are then used to update the temperature and pressure after burning.

Because both pressure and temperature are variables which are not convected in conservation form, but rather are derived from such variables, they are particularly prone to numerical undershoots and overshoots. Consequently, at various places in the code both pressure and temperature are limited so that unrealistic undershoots, in particular, do not occur. Similarly, both f and w are variables which are only defined between the limits zero and one, and so both variables are limited within the code to ensure that these conditions apply. In particular, conditions are imposed so that w remains fixed at one while f is less than one, and f is fixed at one when w is less than one.

The hydrodynamic time step Δt is determined at the start of the integration step via the Courant condition which we use in the form

$$\Delta t = 0.25 \min [\delta x/(|v| + c)] \tag{24}$$

where δx is the computational cell size and c is the sound speed, which is calculated from

$$c^2 = \gamma P/\rho \tag{25}$$

4. Results for $H_2/O_2/Ar$

Our first application of the code is to a stoichiometric mixture of hydrogen and oxygen diluted with argon. The composition of the system is $H_2/O_2/Ar$ in the ratio 2:1:7. This system has been studied extensively at the Naval Research Laboratory using the CHEM0D code and a detailed description of the full kinetic scheme which

converts reactants into products [26]. The time dependence of the reaction has been followed for many values of the initial temperature and pressure and the induction time and rate of energy release have been found to closely follow the expressions given by equations (13) and (14), respectively. The values of the constants A_τ, E_τ, A_r and E_r found by this procedure are given in Table 1. Also shown in Table 1 are the values of the remaining constants which need to be specified for the model, i.e. *mw*, γ and ΔE. As we are using a model in which both *mw* and γ remain fixed during the progress of the reaction, the values we use for these constants when applied to a reaction in which *mw* and γ are different for reactants and products need some consideration. Our only constraint should be that the values we use should lie somewhere between those for the reactants and the products. For our model of $H_2/O_2/Ar$, we have chosen to calculate *mw* and γ for the reactant composition. Taking the molecular weights of H_2, O_2 and Ar to be 2, 32 and 40, respectively, leads to a molecular weight of 31.6 for the reactant mixture. The γ for the reactants is calculated from the expression

$$\gamma = \frac{\sum_{i=1}^{N} n_i C_p}{\sum_{i=1}^{N} n_i C_v} \qquad (26)$$

and leads to the value 1.5555. ΔE is defined as the energy release per unit mass of mixture. The formation of 18 g of H_2O releases 57.8 kcal or 242 kJ of energy. Dilution with argon though results in an energy release of 1.53 kJ/g. This is not the value used for ΔE however as a large fraction of this energy will not be available to drive the detonation, but will instead lead to some degree of dissociation and ionisation of the products. We assume that approximately half the energy released is lost to these processes, and so we take for ΔE a value of 0.75 kJ/g (or 0.178 kcal/g).

The manner in which a steady detonation is initiated in the code is of some importance. In the results we present for $H_2/O_2/Ar$ the code was initiated by depositing an excess amount of energy into a few cells adjacent to the left boundary of the grid. The exact amount of energy, and the number of cells into which it should be deposited, can only be determined by trial and error. A handy rule of thumb is that the excess energy should be approximately five times the energy in the detonation front. For a computational cell size of 4×10^{-4} m, about 10 cells were found to be adequate to initiate detonation. In all the calculations presented here, we imposed rigid wall boundary conditions at either end of the grid.

Table 1: Parameter Values for H_2:O_2:Ar in ratio 2:1:7

A_r	=	24.0×10^8 s^{-1}	mw	=	31.6
E_r	=	3.0×10^4 kcal (12.6×10^4 kJ)	γ	=	1.5555
A_τ	=	5.684×10^{-8} s^{-1}	ΔE	=	3.14 kcal/g^{-1} (13.14 kJ g^{-1})
E_τ	=	1.503×10^4 kcal (6.288×10^4 kJ)			

Figure 1 shows simulation results for this model after 20 000 time steps. The computational grid contained 4 500 cells with $\Delta x = 4.0 \times 10^{-4}$ m and the time step had an average value of 0.05 μs. The detonation was initiated by depositing an excess energy of 3.0×10^6 J per cell into the first 10 cells. The initial temperature and pressure were 300 K and 1.0×10^5 Pa respectively, and the run took approximately 9 hours of VAX 8700 CPU time. The pressure profile shows a very sharp shock front and a jump to a von Neumann point of about 21.5×10^5 Pa. The von Neumann temperature is approximately 1840 K and estimates of the induction time and rate of reaction from equations (13) and (14) using these values indicate that the total reaction zone should span about six computational cells. On the scale of Figure 1, this means that the fall in pressure between the von Neumann point and the CJ point will be compressed into the width of approximately one line, and this explains the sharp spikes displayed by the pressure, density and particle velocity plots, as well as the abrupt transition between zero and one displayed by the reaction variable profile. We estimate the CJ pressure to be 12.4×10^5 Pa, and following this, we observe a Taylor wave expansion down to a steady-state pressure of 4.5×10^5 Pa.

One of the advantages of the model we have described is that analytical results can be compared to the simulation results. Using simple expressions derived in Thompson [35], or Landau and Lifshitz [36], we calculate a CJ velocity for H_2/O_2/Ar of 1542 m/s. Figure 1 also shows detonation velocity versus time. After 5000 time steps (262 μs), the velocity is approximately 1570 m/s, or within 2% of the CJ value. After a further 15 000 time steps (at t = 1050 μs), the velocity has decreased to 1547 m/s, which is 0.3% higher than the CJ value. The estimated CJ pressure of 12.4×10^5 Pa is 1.6% higher than the analytical value of 12.2×10^5 Pa, while the estimated CJ temperature of 2300 K is in very good agreement with the analytical value of 2298 K. A fairly large (approximately 20%) temperature overshoot is evident in the plot of temperature versus computational cell number. Ideally we would expect the temperature to be shocked to the von Neumann point at 1840 K, and then rise again as the reaction proceeds to a peak value of 2300 K at the CJ point. Although both overshoots and undershoots are not unexpected in quantities, the overshoot in temperature observed here is

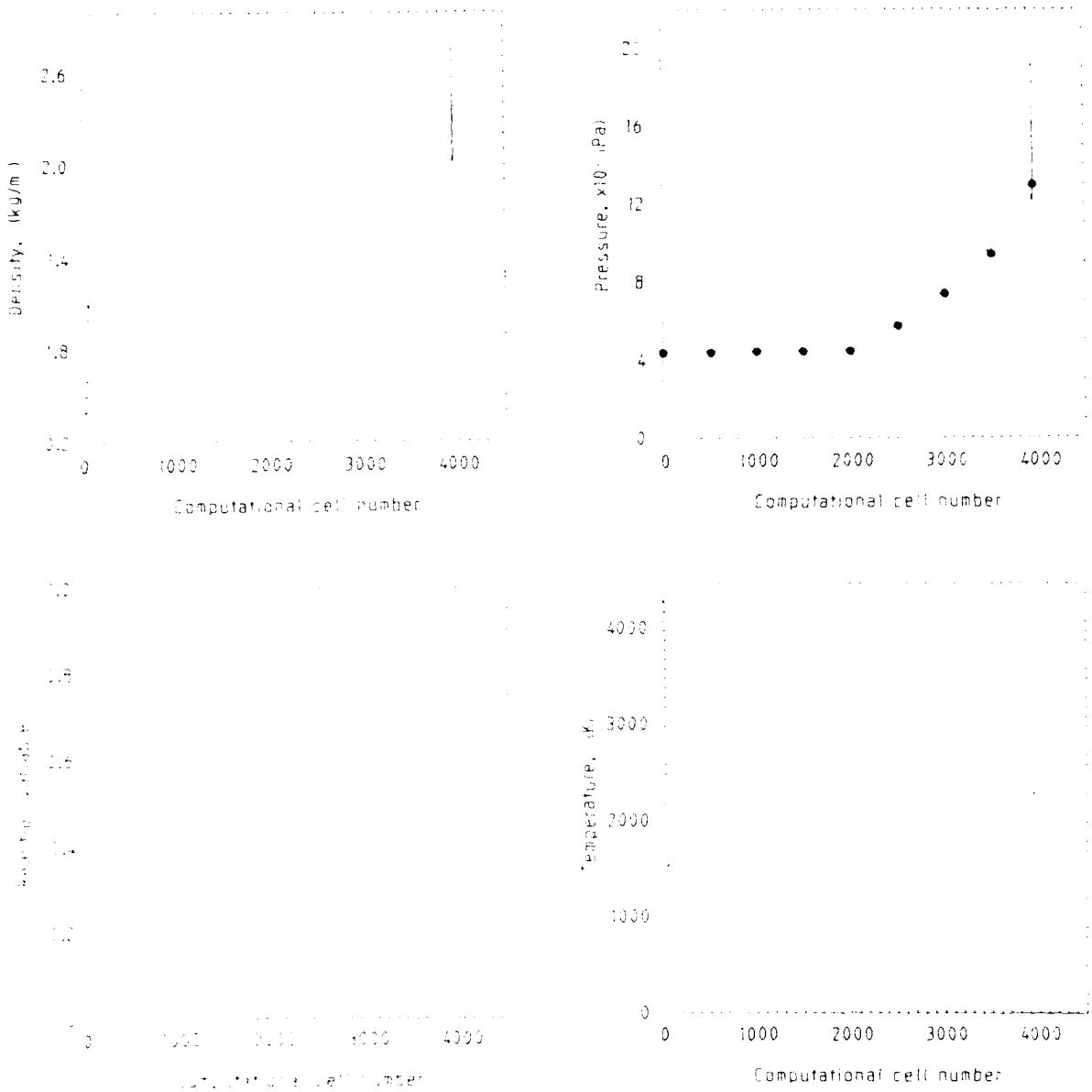

Figure 1: Simulation results for $H_2/O_2/Ar$ after 20 000 time steps. NDUMP = 10, DSTRBO = 3.0×10^6 J and $\Delta x = 4.0 \times 10^{-4}$ m. The filled circles on the pressure and particle velocity profiles are from the self-similar analysis of Kuhl and Seizew [28].

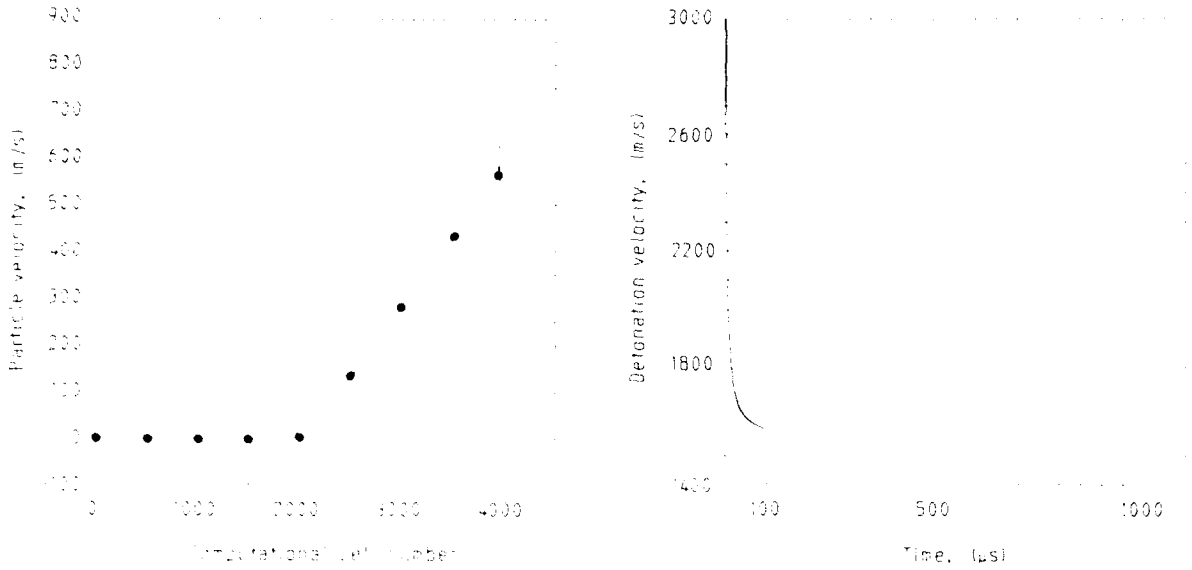

Figure 1 (continued): Simulation results for $H_2/O_2/Ar$ after 20 000 time steps. NDUMP = 10, DSTRBO = 3.0×10^6 J and $\Delta x = 4.0 \times 10^{-4}$ m. The filled circles on the pressure and particle velocity profiles are from the self-similar analysis of Kuhl and Seizew [28].

caused by the narrowness of the reaction zone. We will present results below which show that increasing the number of computational cells within the reaction zone reduces this overshoot. The peak pressure of 21.5×10^5 Pa also undershoots the expected value of 23.9×10^5 Pa by 10% but this is not related to the resolution of the reaction zone; it reflects the limitations of the numerical scheme employed. The other feature worthy of comment is the very high temperature at the left boundary of the grid which is still present after 20 000 time steps. This is a remnant of the extra energy used to initiate the detonation and its slow decay is due to the absence of a heat diffusion term in the model, as well as the zero fluid velocity boundary condition. We will shortly present a different method of initiation which overcomes this problem.

The resolution of Figure 1 is such that the detonation may be viewed as an idealised CJ detonation. In this case the flow field is self-similar and may be calculated using established techniques [27]. Kuhl and Seizew [28] have analysed ideal, strong, CJ detonations using the phase-plane technique and presented tabulated solutions for the flow variables for planar, cylindrical and spherical geometries for detonations in gases ($\gamma = 1.3$) and solids ($\gamma = 2.7$). All properties of the flow field behind strong CJ detonations are functions of the detonation velocity and γ alone (and boundary conditions). Kuhl and Seizew explored the effects of geometry and changes in γ on the computed flow fields and found that pressure and velocity profiles showed only a weak dependence on γ, while density and internal energy profiles showed a pronounced dependence. Hence we can use their tabulated solutions for gases ($\gamma = 1.30$) to analyse our computed pressure and velocity profiles for $H_2/O_2/Ar$ ($\gamma = 1.5555$). The results are shown on the pressure and velocity profiles in Figure 1. The good agreement shows that the 1-D code has accurately calculated the flow field behind the detonation front.

It is important to ensure that the results presented above are independent of the computational cell size. From the excellent agreement shown between the numerical simulation and the analytically calculated CJ parameters and flow fields, we expect that this will be true, but we have also provided a further check by repeating the calculations with computational cell sizes of 2×10^{-4} m, 1×10^{-4} m and 0.5×10^{-4} m. Table 2 summarises the results of these simulations. As a decrease in computational cell size also directly decreases the time step, it is necessary to run for increasingly larger numbers of time steps as the cell size is reduced if the profiles and CJ parameters are to be compared at the same time. We have used a run with $\Delta x = 4 \times 10^{-4}$ m after 2000 time steps (t = 105 μs) for comparison purposes. As Table 2 shows, at t = 105 μs the detonation velocity is still 4% higher than the analytically calculated CJ velocity. These results illustrate in particular the large number of time steps required before the initial disturbance finally decays to a steady-state detonation. The CJ parameters at $t = 105$ μs with $\Delta x = 2 \times 10^{-4}$ m agree almost exactly with those calculated using $\Delta x = 4 \times 10^{-4}$ m. The differences are no more than 2%, except for the von Neumann pressure, where the value calculated using $\Delta x = 2 \times 10^{-4}$ m is closer to the analytical value.

Table 2: Effect of Computational Cell Size H_2:O_2:Ar in ratio 2:1:7

Δx (10^{-4} m)	4.0	2.0	1.0	1.0	0.5	0.5	Analytical
NDUMP	10	20	70	80	220	260	
Number of time steps	2 000	4 000	8 000	8 000	20 000	20 000	
V_{CJ} (m/s)	1 600	1 600	1 640	1 660	1 640	1 680	1542.0
P_{CJ} (10^5 Pa)	12.8	13.0	14.4	14.5	14.5	15.8	12.2
T_{CJ} (K)	2350	2360	2450	2500	2500	2590	2298
P_{VN} (10^5 Pa)	20.7	22.0	22.8	24.0	23.2	22.5	24.4
T_{max}	2780	2780	2700	2700	2500	2590	2298

t = 105 μs for $\Delta x = 4.0 \times 10^{-4}$ m, 2.0×10^{-4} m and 1.0×10^{-4} m, and 131.3 μs for $\Delta x = 0.5 \times 10^{-4}$ m.

NDUMP = 3.0×10^6 Joules/cell in each case.

It is of interest to examine the profiles of the flow variables in the case where insufficient energy is deposited in the system and the detonation dies. This is illustrated in Figure 2, which shows pressure, temperature, and reaction-variable profiles at two different times for a simulation with $\Delta x = 2 \times 10^{-4}$ m, DSTRBO = 3.0×10^6 J, and NDUMP = 10. The pressure and temperature profiles at $t = 105$ μs show that the shock front is located at cell number 600, while the reaction front is located near cell number 330. At $t = 210$ μs the shock front is located at cell number 1100, while the reaction front is located near cell 400. This separation of the reaction front from the shock front is typical of an explosive event which fails to establish itself as a propagating detonation. The shock front velocity versus time is also shown in Figure 2.

Another interesting case is shown in Figure 3. Parameter values used are $\Delta x = 0.5 \times 10^{-4}$ m, DSTRBO = 3.0×10^6 J, and NDUMP = 260. The pressure and reaction variable profiles after 4 000 time steps are typical of those of a decaying reactive shock, and at this stage a self-sustaining detonation has not been initiated. After a further 1 200 time steps however the shock front and reaction front have become strongly coupled and an overdriven self-sustaining detonation has been established. The point at which this occurs is evident in the velocity versus time plot.

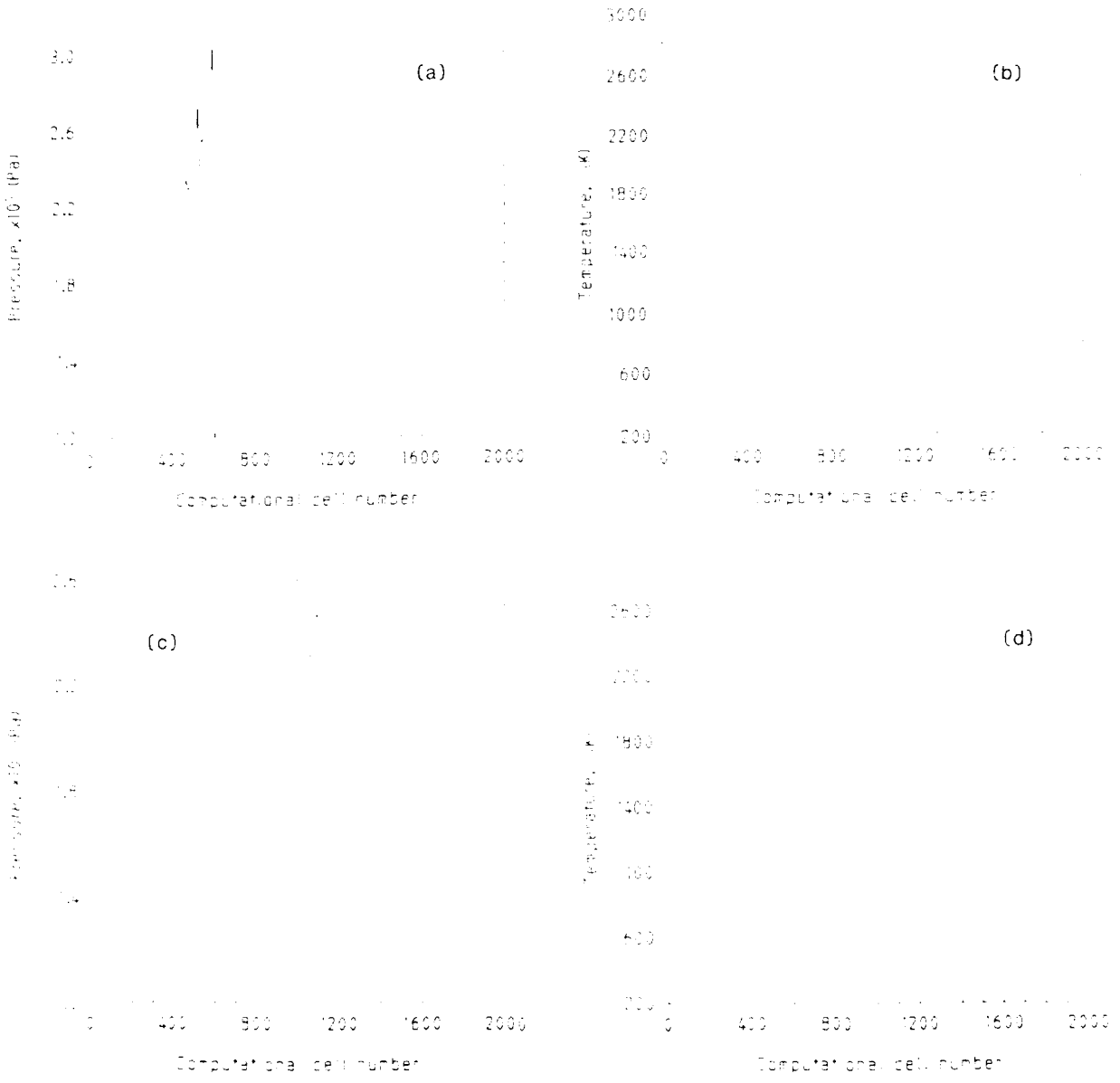

Figure 2: Pressure, temperature and reaction variable profiles at t = 105 μs (a, b and e) and t = 210 μs (c, d and f) for $H_2/O_2/Ar$. NDUMP = 10, DSTRBO = 3.0×10^6 J and $\Delta x = 2.0 \times 10^{-4}$ m. Shock front velocity versus time also shown (g).

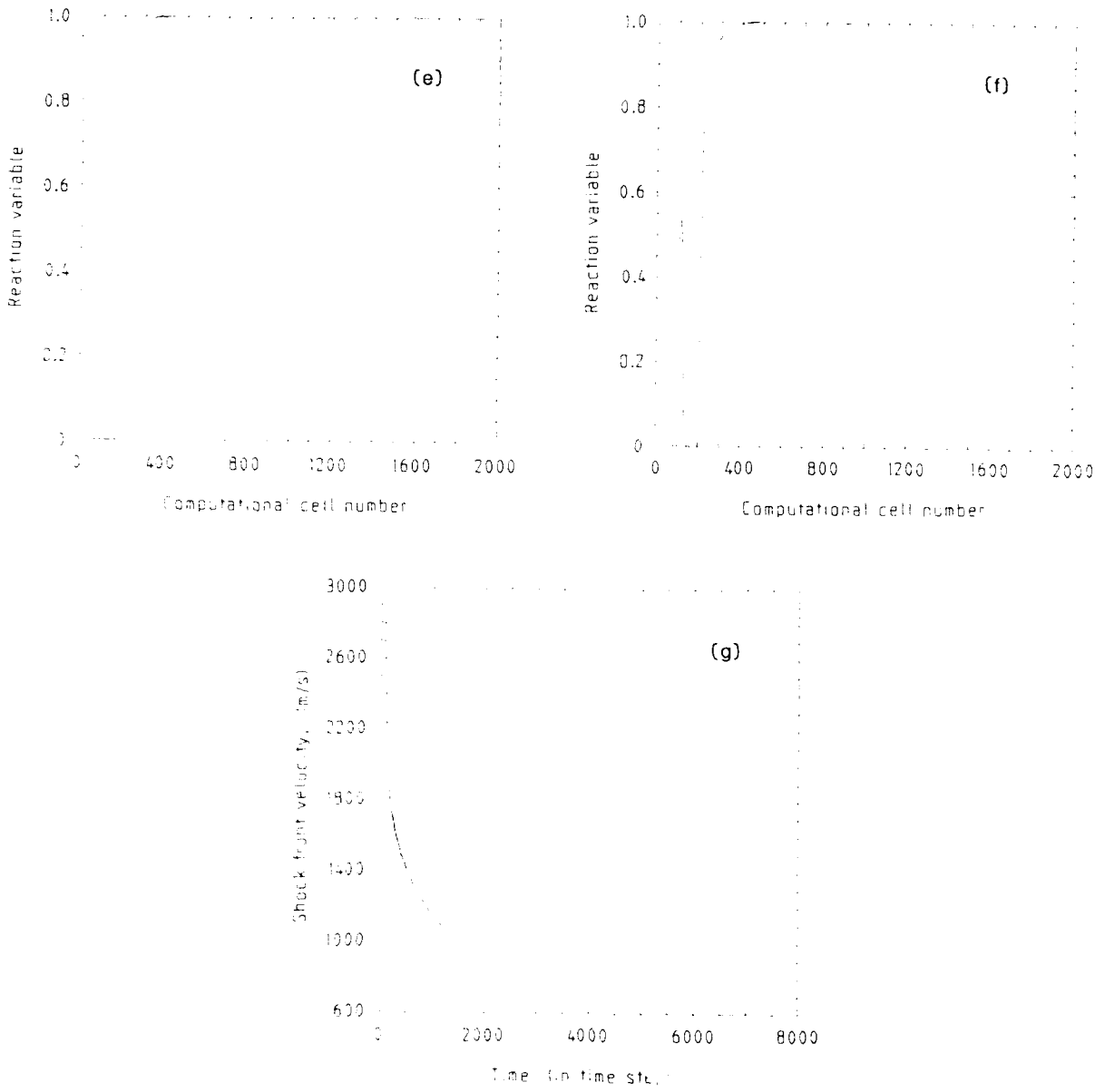

Figure 2 (continued): Pressure, temperature and reaction variable profiles at t = 105 μs (a, b and e) and t = 210 μs (c, d and f) for $H_2/O_2/Ar$. NDUMP = 10, DSTRBO = 3.0×10^6 J and $\Delta x = 2.0 \times 10^{-4}$ m. Shock front velocity versus time also shown (g).

5. Results for Stoichiometric H_2/O_2

The model for H_2/O_2/Ar just described has recently been used in a two-dimensional, two-species reactive code to model the transfer of detonation between gaseous explosive layers [29-31]. These simulations were performed to model experiments conducted at the University of Michigan using gaseous mixtures of hydrogen and oxygen of varying equivalence ratios [32, 33]. While the simulations provided good qualitative agreement with the experimental results, they were unable to provide a quantitative comparison because of differences between the explosive mixtures used in the experiments and in the simulations. In order to better reproduce the experimental results, we have slightly altered the model for H_2/O_2/Ar which has just been described so that it can simulate detonation in a stoichiometric mixture of gaseous hydrogen and oxygen. In this section we describe how the constants for the model are derived and then display typical results of flow-field simulations. We also describe a slightly different method of initiation which appears to be more efficient than the one used to initiate the H_2/O_2/Ar mixture.

The important quantities to be determined are the rate of energy release and induction time as a function of pressure and temperature, and the molecular weight, gamma, and total amount of energy released. The induction time and rate of energy release were calculated using the CHEM0D code and the full set of elementary reaction steps for the hydrogen-oxygen reaction. Details of the integration routines used in CHEM0D are described in reference [17]. A CJ detonation in a stoichiometric mixture of hydrogen and oxygen at an initial pressure of one atmosphere and a temperature of 300 K has a Mach number of 5.2822 (determined from the Gordon-McBride code [34]). This allows us to calculate a von Neumann pressure and temperature of 32.4×10^5 Pa and 1822 K respectively. The CHEM0D code was therefore run over a range of initial pressures and temperatures around these values. Runs were made for initial pressures of 5, 20, 30 and 50×10^5 Pa for initial temperatures between 1500 K and 2000 K. We found the time dependence of the energetics of the stoichiometric mixture to be much simpler than the argon diluted mixture, and virtually independent of initial temperature and pressure. Each of the temperature versus time curves in the region of interest was characterised by a constant induction time of approximately 2×10^{-7} s, followed by a rapid increase in temperature until approximately 90% of the energy had been released, then a slower increase until levelling off at a constant value. The time interval between the initial rapid rate of temperature rise and the final constant temperature was found to be approximately constant and to have a value of 5×10^{-7} s. This time dependence is well represented by using a reaction rate law of the form

$$\frac{1}{w}\frac{dw}{dt} = -\frac{1.0}{5 \times 10^{-7}\ s} \qquad (27)$$

coupled to a constant induction time of 2×10^{-7} s.

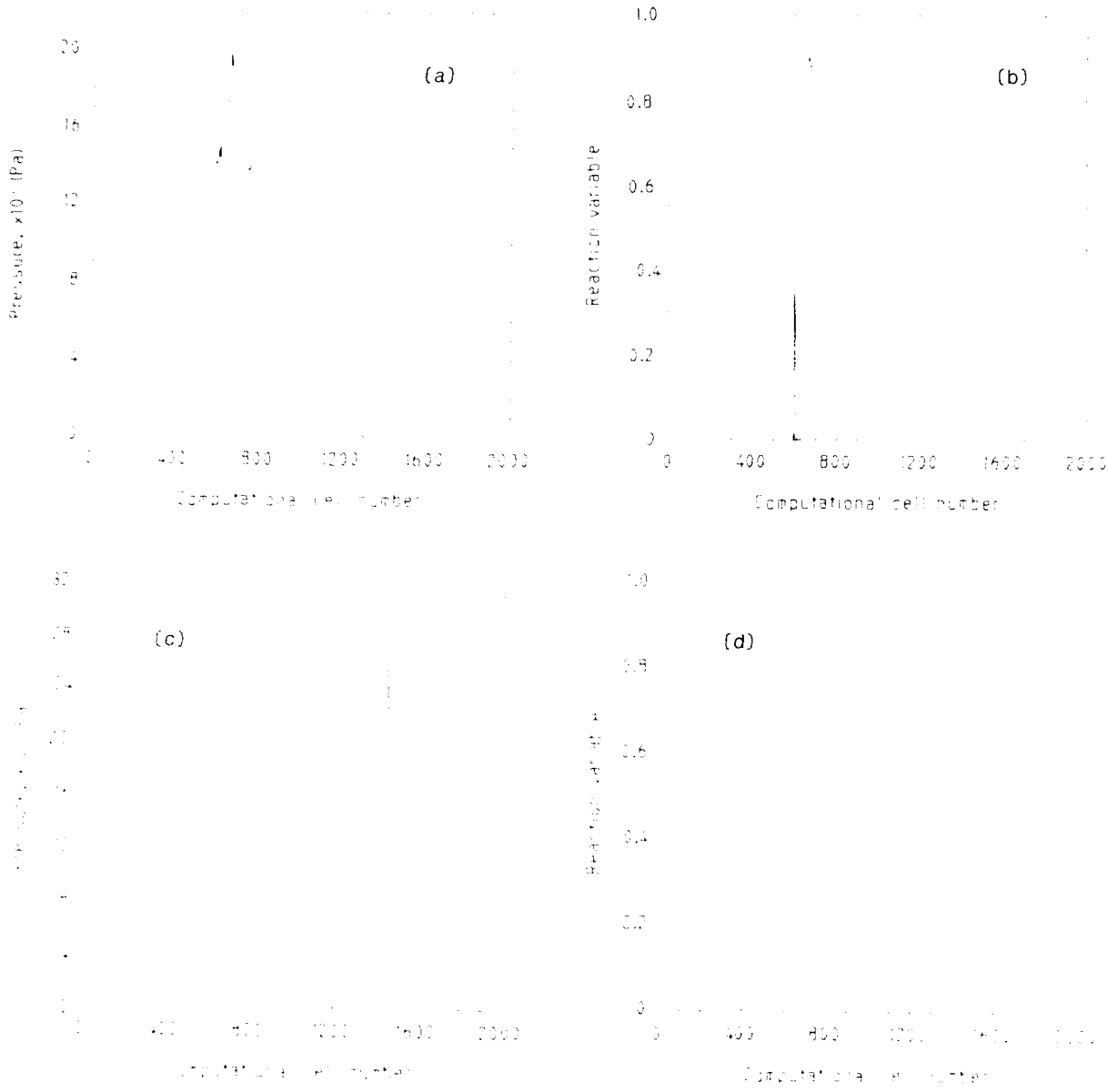

Figure 3: Pressure and reaction variable profiles at t = 4 000 (a and b) and t = 8 000 (c and d) time steps for H_2/O_2/Ar. NDUMP = 260, DSTRBO = 3.0×10^6 J and $\Delta x = 0.5 \times 10^{-4}$ m. Shock front velocity versus time also shown (e). These diagrams illustrate the formation of an overdriven detonation from an initially decaying reactive shock.

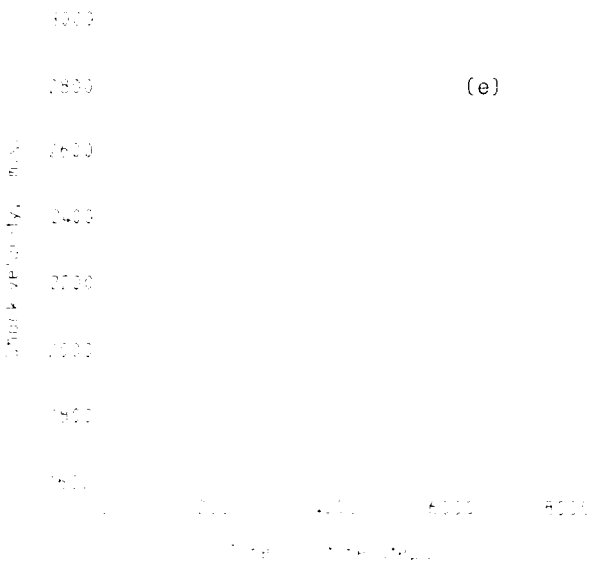

Figure 3 (continued): Pressure and reaction variable profiles at t = 4 000 (a and b) and t = 8 000 (c and d) time steps for H_2, O_2/Ar. NDUMP = 260, DSTRBO = 3.0 × 10^6 J and Δx = 0.5 × 10^{-4} m. Shock front velocity versus time also shown (e). These diagrams illustrate the formation of an overdriven detonation from an initially decaying reactive shock.

Three quantities remain to be determined; *mw*, γ, and ΔE. Rather than try to estimate these from averages over appropriate values for reactants or products as we did for H_2/O_2/Ar, we adopted a different approach. Our primary objective in the development of this model for stoichiometric H_2/O_2 was to accurately simulate a steadily propagating CJ detonation. In particular, we required our simulation to accurately reproduce the CJ velocity, pressure and temperature. Hence we treated *mw*, γ, and ΔE as variables (within appropriate limits), and used analytical expressions to find values for these variables which reproduce the CJ parameters. For stoichiometric H_2/O_2 the Gordon-McBride code calculates the CJ parameters to be V_{CJ} = 2800 m/s, $P_{CJ} = 18.0 \times 10^5$ Pa, and T_{CJ} = 3600 K. We were unable to reproduce these values exactly by varying *mw*, γ, and ΔE, but found that the choice of *mw* = 13.2, γ = 1.37, $\Delta E = 4.2 \times 10^6$ J/kg gave analytical values of V_{CJ} = 2800 m/s, $P_{CJ} = 18.0 \times 10^5$ Pa, and T_{CJ} = 3200 K.

In modelling the experimental results the more important variables to simulate accurately are the detonation velocity and pressure, and we expect the 11% discrepancy in CJ temperature to have little effect on the value of these variables. Hence we have adopted the parameter values described above, and collected them together in Table 3 for reference.

Following discussions with K. Kailasanath of the Naval Research Laboratory, we have also used a different method of initiation for stoichiometric H_2/O_2. The procedure we follow is to first calculate the initial shock pressure and temperature assuming that the material is non reactive; these are the von Neumann values, which we have already calculated to be $P_{VN} = 32.4 \times 10^5$ Pa and $T_{VN} = 1822$ K. Rather than deposit a fairly large amount of energy into NDUMP cells at $t = 0$ we now simply set the pressure and temperature to the von Neumann values. Even with the initial fluid velocity in these cells set to zero this is sufficient to initiate a stable, propagating detonation. The advantage of this method is that less excess energy is deposited initially so the system approaches the steady state more quickly. Another advantage is that it removes the unphysically high temperature which persists at the boundary long after the initial deposition of energy.

Table 3: Parameter Values for Stoichiometric H_2/O_2

Induction time : $\tau = 2 \times 10^{-7}$ s
Reaction Rate law : 1/w dw/dt = - 1.0 / (5×10^{-7} s)
mw = 13.2
γ = 1.37
$\Delta E = 4.2 \times 10^6$ Joules/kg
Analytical CJ values from above constants:
V_{CJ} = 2800 m/s
$P_{CJ} = 18.0 \times 10^5$ Pa
T_{CJ} = 3200 K

Figure 4 shows pressure, temperature and velocity profiles for stoichiometric H_2/O_2 after 20 000 time steps, or $t = 560$ μs. We used $\Delta x = 4 \times 10^{-4}$ m and NDUMP = 3. The shock velocity versus time is also shown. The pressure and velocity profiles are similar to those for H_2/O_2/Ar in Figure 1 and show the same self-similarity behaviour. The temperature profile is also similar, but the different method of initiation has resulted in much more realistic behaviour at the left boundary where the initial disturbance was applied. Also shown in Figure 4 is the detonation velocity versus time, which shows that the velocity has reached a steady state value of approximately 2807 m/s after only 4000 time steps. The CJ pressure estimated from Figure 4 is 18.0×10^5 Pa and the CJ temperature is 3. 00 K. The analytically calculated values for the parameters used in the model are 2800 m/s, 18.0×10^5 Pa and 3200 K respectively. The peak pressure of 29.2×10^5 Pa is 10% lower than the von Neumann value of 32.4×10^5 Pa, and there is still a large temperature overshoot of approximately 10%.

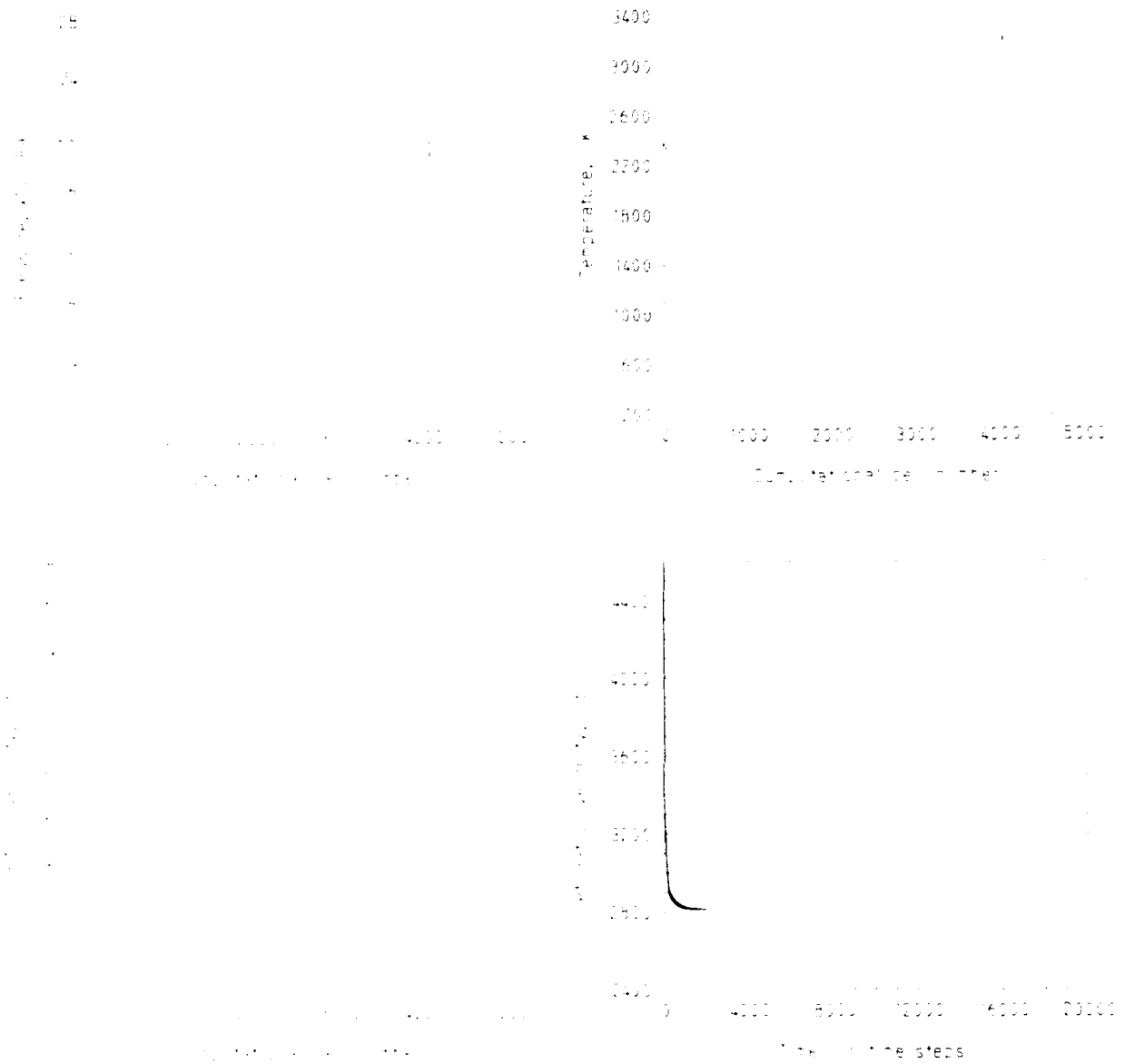

Figure 4: Pressure, temperature and particle velocity profiles for stoichiometric H_2/O_2 at t = 560 μs. $\Delta x = 4.0 \times 10^{-4}$ m and NDUMP = 3. Detonation velocity versus time also shown. These diagrams are similar to those in Figure 1 for $H_2/O_2/Ar$, but in this case both the induction time and rate of energy release is constant. A different method of initiation has also been used.

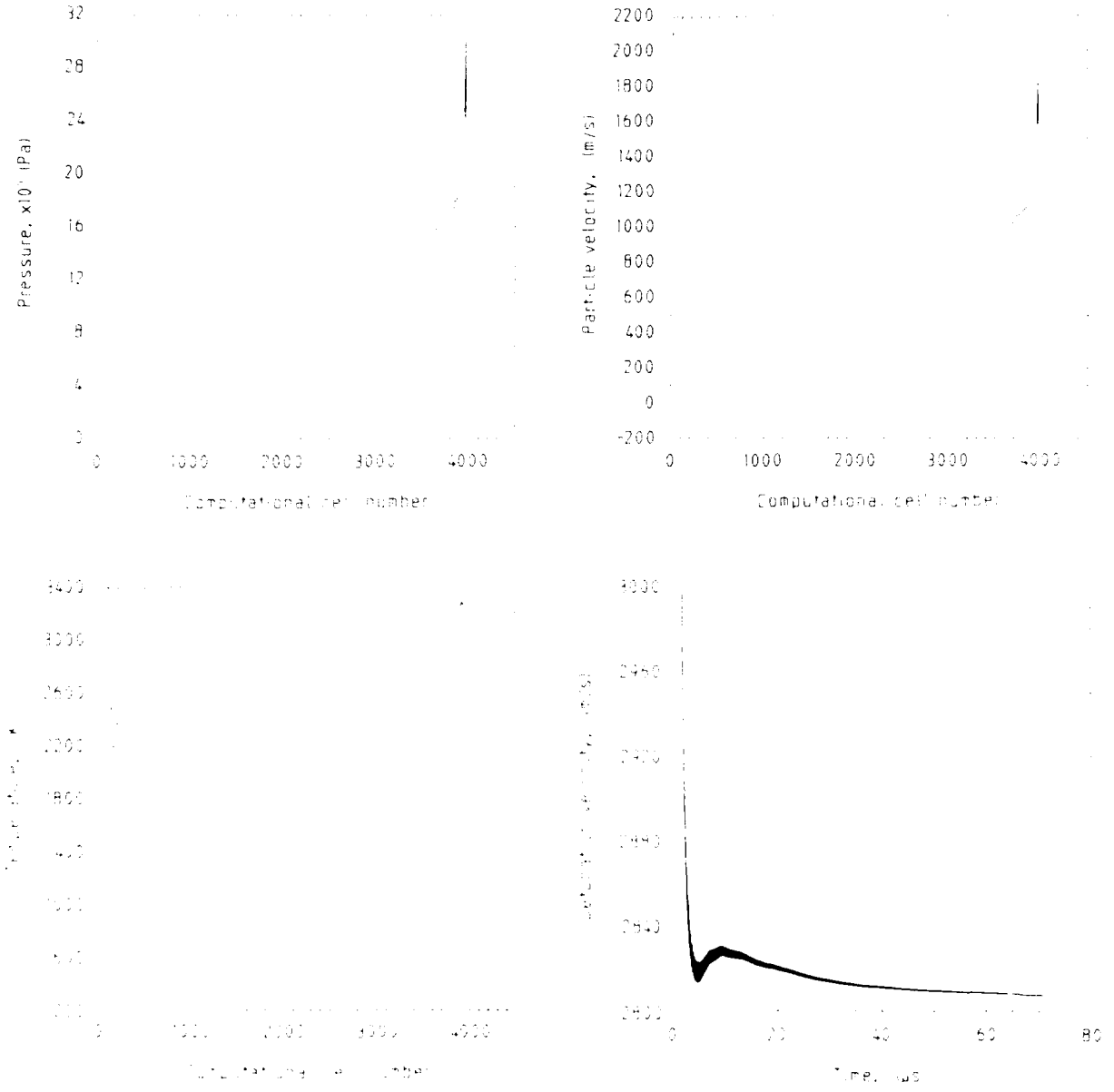

Figure 5: Pressure, temperature and particle velocity profiles for stoichiometric H_2/O_2 at t = 70 μs. $\Delta x = 0.5 \times 10^{-4}$ m and NDUMP = 25. Detonation velocity versus time also shown. These diagrams show the same flow variables as the previous Figure, but in this case there are eight times as many computational cells in the reaction zone.

We have repeated these simulations using computational cell sizes of 2×10^{-4} m, 1×10^{-4} m, and 0.5×10^{-4} m to again check for any dependence of the results on cell size. Figure 5 shows pressure, temperature and velocity profiles calculated using $\Delta x = 0.5 \times 10^{-4}$ m after 20 000 time steps, corresponding to $t = 70$ μs. The profiles are very similar to the ones calculated using $\Delta x = 4 \times 10^{-4}$ m, the only difference occurs in the peak values of the variables. The peak pressure is now approximately 31.5×10^5 Pa, or only 3% lower than the von Neumann value, and the temperature overshoot has been reduced to approximately 2%. The detonation velocity versus time curve again shows the velocity approaching a value of 2807 m/s. We used NDUMP = 25 for this run and the detonation velocity curve shows that this was just sufficient to initiate detonation. The thickness of the curve is due to a very rapid oscillation which is too fine to resolve on the scale shown. This oscillation is not physical but is caused by the "step like" position versus time profile displayed by the shock front. The Courant condition forces the shock to take approximately five or six time steps to traverse a computational cell, which means that the velocity continuously decreases for five or six steps and then instantly jumps back to a value slightly below the value it had at the start of the cycle. These oscillations are also present in the detonation velocity plot in Figure 1, but are too fine to be seen on that scale.

The reduction in the temperature overshoot which has been achieved by using a much smaller computational cell size can also be achieved with larger cell sizes if the reaction zone is limited to a minimum width. The temperature profile in Figure 6a has been calculated using $\Delta x = 4.0 \times 10^{-4}$ m and a temperature correction of the form

$$T_i = \min\,(T_{i-1}, T_i, T_{i+1}) \tag{28}$$

As can be seen by comparison with Figure 4, the use of equation (28) has reduced the overshoot from 8.8% to 3.8%. The temperature profile in Figure 6b is also for stoichiometric H_2/O_2 with $\Delta x = 4.0 \times 10^{-4}$ m but using a stronger limitation of the form

$$T_i = \min\,(T_{i-2}, T_{i-1}, T_i, T_{i+1}, T_{i+2}) \tag{29}$$

This reduces the overshoot to less than 1%. Figure 7 shows the result of applying equation (28) to $H_2/O_2/Ar$ with $\Delta x = 4.0 \times 10^{-4}$ m. Comparison with Figure 1 again shows a reduction in overshoot from around 20% to approximately 1%. It is important to note that use of equation (28) on (29) does not introduce any changes in the other variables in the simulation, and the only effect on the temperature profile is the significant reduction in the magnitude of the temperature overshoot.

We have also investigated the effect of the number of cells used for initiation, NDUMP, and the total number of time steps, MAXSTP, on our estimates of the CJ parameters. The results are shown in Table 4 for the fixed computational cell size

of $\Delta x = 4 \times 10^{-4}$ m. We used the induction time and reaction rate expression derived for stoichiometric H_2/O_2, but slightly different values for γ, *mw* and ΔE. The results are as expected, increasing MAXSTP and decreasing NDUMP lead to increasingly more accurate estimates of the CJ parameters. The table does illustrate the asymptotic nature of the converge, with very large increases in MAXSTP required to gain very small decreases in the percentage error.

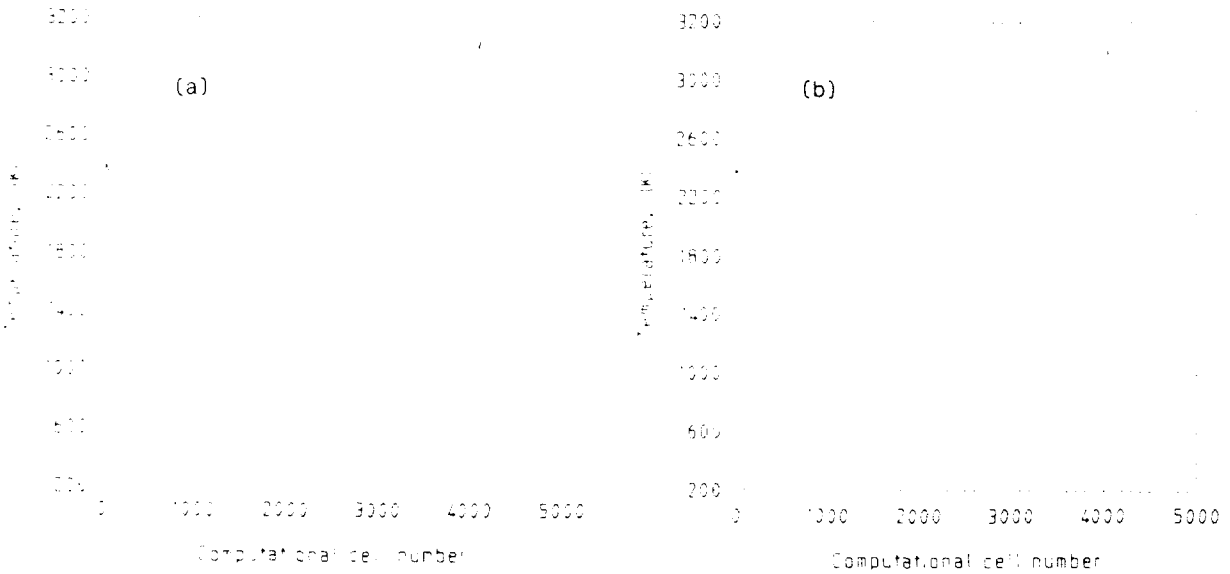

Figure 6: Temperature profiles for stoichiometric H_2/O_2. $\Delta x = 4.0 \times 10^{-4}$ m, NDUMP = 3 and ISTEP = 20 000. Reaction zone limited to a minimum width using $T_i = min\ (T_{i-1}, T_i, T_{i+1})$ in Figure 6a, and $T_i = min\ (T_{i-2}, T_{i-1}, T_i, T_{i+1}, T_{i+2})$ in Figure 6b. The reduction in temperature overshoot obtained by these prescriptions is clearly evident.

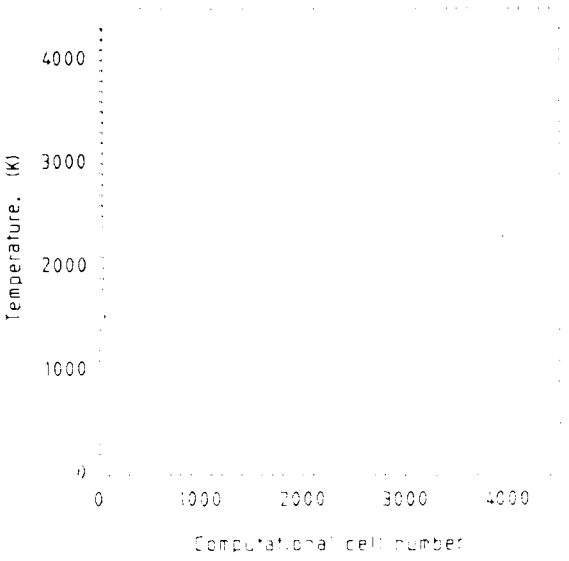

Figure 7: Temperature profile for $H_2/O_2/Ar$. $\Delta x = 4.0 \times 10^{-4}$ m, NDUMP = 10, DSTRBO = 3.0×10^6 J, ISTEP = 20 000. Reaction zone limited to a minimum width using $T_i = min\ (T_{i-1}, T_i, T_{i+1})$. Comparison with the temperature profile in Figure 1 shows that the above simple limiting procedure has completely eliminated the temperature overshot.

Table 4: Effect of MAXSTP and NDUMP on accuracy of estimates of CJ parameters

MAXSTP	1 000	8 000	20 000	1 000	20 000	Analytical
NDUMP	10	10	10	5	5	
V_{CJ} (m/s)	2 800	2 680	2 666	2 700	2 650	2 650
P_{CJ} (10^5 Pa)	23.5	20.0	19.0	20.5	18.1	18.4
T_{CJ} (K)	3 500	3 300	3 280	3 300	3 230	3 245

NOTE: Second method of initiation used

$\gamma = 1.35$, mw = 15.0, $\Delta E = 4.0 \times 10^6$

6. Conclusion

The results discussed in the previous section demonstrate the effectiveness of the computer code described in this report. The code has been used to simulate steadily propagating detonations in stoichiometric mixtures of H_2 and O_2, and also H_2/O_2 mixtures diluted with Ar. The results of the simulations agree well with variable profiles calculated from solutions using self-similarity analysis, and the CJ parameters estimated from the profiles agree well with values calculated from analytical expressions. The CJ parameters are independent of the computational cell size, and both the undershoot in calculated peak pressure and overshoot in calculated peak temperature decrease with increasing grid resolution in the reaction zone. The effect of the method of initiation, and number of time steps included in the simulation, on the accuracy of the results has also been investigated.

We anticipate that replacement of the polytropic equation of state by the HOM equation of state, described by Mader [1], and replacement of the first order Arrhenius kinetics by a more sophisticated description of the material decomposition, such as the one described by Kim and Sohn [6], will enable particle size effects in condensed phase heterogeneous explosives to be investigated.

7. Acknowledgements

This work was started while D.A. Jones was a Visiting Scientist funded by MRL under the US-Australia DOD Scientist Engineer Exchange Program at the Laboratory for Computational Physics and Fluid Dynamics at the Naval Research Laboratory, Washington, DC. He wishes to thank Dr Jay P. Boris, Chief Scientist and Director of LCP and FD, for the opportunity to work in such a stimulating environment, and for the provision of excellent computing and support facilities. We thank Dr K. Kailasanath of LCP and FD for several very helpful discussions, as well as running the CHEM0D code for the stoichiometric H_2/O_2 data. We have also benefited greatly from discussions and correspondence with Professor Martin Sichel of the University of Michigan, Ann Arbour, MI.

8. References

1. Mader, C.L. (1979).
Numerical modelling of detonation. University of California Press.

2. Fickett, W. and Davis, W.C. (1979).
Detonation. Berkeley: University of California Press.

3. Hubbard, H.W. and Johnson, M.H. (1959).
Initiation of detonations. *Journal of Applied Physics*, **30**, 765-769.

4. von Neumann, J. and Richtmyer, R.D. (1950).
Journal of Applied Physics, **21**, 232.

5. Fickett, W. and Wood, W.W. (1966).
Flow calculations for pulsating one-dimensional detonations. *Physics of Fluids*, **9**, 903-916.

6. Kim, K. and Sohn, C.H. (1985).
Modelling of reaction buildup processes in shocked porous explosives. *Eighth Symposium (International) on Detonation*, Albuquerque, New Mexico, July 1985, p. 926-933.

7. Jones, D.A. (1989).
An assessment of burn models available for implementation in a computer code to model shock initiation of heterogeneous explosives (MRL Technical Report MRL-TR-89-17). Maribyrnong, Vic: Materials Research Laboratory.

8. Boris, J.P. and Book, D.L. (1973).
Flux-corrected transport. I. SHASTA, A fluid transport algorithm that works. *Journal of Computational Physics*, **11**, 38-69.

9. Book, D.L., Boris, J.P. and Hain, K. (1975).
Flux-corrected transport. II. Generalizations of the method. *Journal of Computational Physics*, **18**, 248-283.

10. Boris, J.P. and Book, D.L. (1976).
Flux-corrected transport. III. Minimal-error FCT algorithms. *Journal of Computational Physics*, **20**, 397-431.

11. Sod, G.A. (1978).
A survey of several finite difference methods for systems of nonlinear hyperbolic conservation laws. *Journal of Computational Physics*, **27**, 1-31.

12. Kailasanath, K. and Oran, E.S. (1983).
Ignition of flamelets behind incident shock waves and the transition to detonation. *Combustion Science and Technology*, **34**, 345-362.

13. Kailasanath, K., Oran, E.S. and Boris, J.P. (1985).
Determination of detonation cell size and the role of transverse waves in two-dimensional detonations. *Combustion and Flame*, **61**, 199-209.

14. Guirguis, R. and Oran, E.S. (1983).
Reactive shock phenomena in condensed materials: Formulation of the problem and method of solution (NRL Memorandum Report 5228). Washington, DC: Naval Research Laboratory.

15. Guirguis, R., Oran, E.S. and Kailasanath, K. (1986).
Numerical simulations of the cellular structure of detonations in liquid nitromethane - regularity of the cell structure. *Combustion and Flame*, **65**, 339-366.

16. Guirguis, R., Oran, E.S. and Kailasanath, K. (1987).
The effect of energy release on the regularity of detonation cells in liquid nitromethane. *Proceedings of the 21st Symposium (International) on Combustion*, The Combustion Institute, Pittsburgh, PA.

17. Oran, E.S. and Boris, J.P. (1987).
Numerical simulation of reactive flow. Elsevier Science Publishing Co. Inc.

18. Nunziato, J.W. and Baer, M.R. (1988).
Flame propagation and growth to detonation in multiphase flows. *Computational fluid dynamics and reacting gas flows*, Springer-Verlag, 257-289.

19. Thomas, G.O. (1989).
Private communication.

20. Davis, W.C. (1980).
High explosives - The interaction of chemistry and mechanics. *Los Alamos Science*, **1**, 49-75.

21. Callen, H.B. (1960).
Thermodynamics. John Wiley and Sons Inc.

22. Menikoff, R. and Plohr, B.J. (1989).
The Riemann problem for fluid flow of real materials. *Reviews of Modern Physics*, **61**, 75-130.

23. Fickett, W. (1985).
Detonation in miniature. In J.D. Buckmaster (Ed.) *The Mathematics of Combustion, Vol. 2 of Frontiers in Applied Mathematics* (Society for Industrial and Applied Mathematics, Philadelphia), p. 133-181.

24. Oran, E., Boris, J.P., Young, T.R. and Picone, J.M. (1981).
Numerical simulations of detonations in hydrogen-air and methane-air mixtures. *Proceedings of the 18th Symposium (International) on Combustion*, The Combustion Institute, Pittsburgh, PA, pp. 1641-1649.

25. Boris, J.P. (1976).
Flux-corrected transport modules for solving generalized continuity equations (NRL Memorandum Report 3237). Washington, DC: Naval Research Laboratory.

26. Oran, E.S. and Boris, J.P. (1982).
Weak and strong ignition. II. Sensitivity of the hydrogen-oxygen system. *Combustion and Flame*, **48**, 149-161.

27. Zeldovich, Ya. B. and Raiser, Yu. P. (1966).
Physics of shock waves and high-temperature hydrodynamic phenomena.
Ed. W.D. Hayes and R.F. Probstein, Vol. II, pp. 785-863.

28. Kuhl, A.L. and Seizew, M.R. (1978).
Analysis of ideal, strong, Chapmann-Jouquet detonations (TRW Report 78.4735.9-13).

29. Jones, D.A., Guirguis, R. and Oran, E.S. (1989).
Numerical simulation of detonation transfer between gaseous explosive layers (MRL Research Report MRL-RR-1-89). Maribyrnong, Vic: Materials Research Laboratory.

30. Jones, D.A., Sichel, M., Guirguis, R. and Oran, E.S. (1990).
Numerical simulation of layered detonations, to appear in *Progress in Aeronautics and Astronautics*, AIAA, Washington.

31. Sichel, M., Jones, D.A., Oran, E.S. and Guirguis, R. (1990).
Detonation transmission in layered explosives, to appear in *Proceedings of the 23rd Symposium (International) on Combustion.*

32. Liu, J.C., Sichel, M. and Kauffman, C.W. (1987).
The lateral interaction of detonating and detonable gaseous mixtures. To appear in *Progress in Astronautics and Aeronautics, 1988, Proceedings of the 11th International Colloquium on the Dynamics of Energetic and Reactive Systems.*

33. Liu, J.C., Liou, J.J., Sichel, M., Kauffman, C.W. and Nicholls, J.A. (1987).
Diffraction and transmission of a detonation into a bounding explosive layer. *Proceedings of the 21st Symposium (International) on Combustion*, pp. 1659-1668. The Combustion Institute, Pittsburg, PA.

34. Gordon, S. and McBride, B.J.
Computer program for calculation of complex chemical equilibrium compositions, rocket performance, incidental and reflected shocks, and Chapman-Jouquet detonations (NASA SP-273). NASA, Washington, DC.

35. Thompson, P.A. (1972).
Compressible fluid dynamics. McGraw-Hill Book Company.

36. Landau, L.D. and Lifshitz, J.M. (1959). *Fluid mechanics.* Pergamon Press.

SECURITY CLASSIFICATION OF THIS PAGE **UNCLASSIFIED**

DOCUMENT CONTROL DATA SHEET

REPORT NO.	AR NO.	REPORT SECURITY CLASSIFICATION
MRL-RR-2-90	AR-006-336	Unclassified

TITLE

A one dimensional flux-corrected transport code for detonation calculations

AUTHOR(S)

D.A. Jones, E.S. Oran and
R. Guirguis

CORPORATE AUTHOR

DSTO Materials Research Laboratory
PO Box 50
Ascot Vale Victoria 3032

REPORT DATE	TASK NO.	SPONSOR
March, 1991	88/090	

FILE NO.	REFERENCES	PAGES
G6/4/8-3854	36	37

CLASSIFICATION/LIMITATION REVIEW DATE

CLASSIFICATION/RELEASE AUTHORITY
Chief, Explosives Division

SECONDARY DISTRIBUTION

Approved for public release

ANNOUNCEMENT

Announcement of this report is unlimited

KEYWORDS

Numerical simulation
Flux-corrected transport
Reactive shock
Detonation

ABSTRACT

The development of a one-dimensional Flux-Corrected Transport code to model detonation in a homogeneous medium is described. The material flow is modelled using the Euler equations, and the chemical kinetics by a two-step induction parameter model which uses a quasi-steady induction time and first order Arrhenius kinetics. Two different modes of initiation are tried and compared. Conditions necessary for a self-sustaining detonation are described and illustrated. A detailed comparison is made between the variable profiles calculated by the code and those calculated analytically using the simple Chapman-Jouguet theory and self-similar analysis, and the overall agreement is excellent. The effect of the computational cell size on these solutions is also considered.